EXPANDING THE CONCEPTUAL MODEL FOR THE CARTER CAVES SYSTEM, CARTER COUNTY, KENTUCKY USING GIS

Lara E. Harlan

68 Pages August 2009

This research used GIS to model the stream network, watershed, sinkholes, lineaments, and elevations of cave entrances to describe distinct layers within a cave system.

APPROVED:

_____

Date Eric W. Peterson, Chair

_____

Date John Kostelnick

_____

Date Toby Dogwiler

EXPANDING THE CONCEPTUAL MODEL FOR THE CARTER CAVES SYSTEM, CARTER COUNTY, KENTUCKY USING GIS

Lara E. Harlan

68 Pages August 2009

Carter Caves State Resort Park (CCSRP) in northeastern Kentucky has been studied for years but yet little is known about the layers within the cave system. Karstic systems can be complicated by the development of layers within the system. Elevations of caves are used to help identify the layers within a karst system. In GIS software, a digital elevation model (DEM), raster data representing elevations for a given area, can be used to obtain elevation data and help delineate the layers within a system. Using the location data collected by Wittenberg University, elevations for cave entrances were extracted from a DEM and then compared to the field elevations obtained by Winona State University. In order to explain these layers through a conceptual model several other factors (stream network, watershed, lineaments, and sinkholes) were examined. The CCSRP contains many sinking streams, which masks the stream network. The streams in the park seem fragmented, not connected and the stream network is not obvious. Using ESRI's ArcMap, a Stream Network Model was created using sub routines to delineate the stream network from a DEM. The resulting stream networks were compared to the KGS stream data to calibrate

the model. The stream network model showed that the streams in and around the CCSRP are continuous over the area even though they are not entirely expressed at the surface and have a greater area of influence of erosion on the rocks below. In general, the closer a cave entrance was to the stream network, the lower in elevation it was and vice versa, the further away, the higher the elevation. As the streams incised into bedrock the cave entrances moved further away from the stream. Thus, the number of layers within the CCSRP shows that this area has experienced many changes in the stability of the water table. In addition, the rivers contained within the park have rapidly down cut through the bedrock and have stalled out several times before reaching the elevations that they are seen at today.

APPROVED:

_____

Date Eric W. Peterson, Chair

_____

Date John Kostelnick

_____

Date Toby Dogwiler

EXPANDING THE CONCEPTUAL MODEL FOR THE CARTER CAVES SYSTEM, CARTER COUNTY, KENTUCKY USING GIS

LARA E. HARLAN

Thesis Submitted in Partial
Fulfillment of the Requirements
for the Degree of

MASTER OF SCIENCE

Department of Geography-Geology

ILLINOIS STATE UNIVERSITY

2009

EXPANDING THE CONCEPTUAL MODEL FOR THE CARTER CAVES SYSTEM, CARTER COUNTY, KENTUCKY USING GIS

LARA E. HARLAN

APPROVED:

_____

Date Eric W. Peterson, Chair

_____

Date John Kostelnick

_____

Date Toby Dogwiler

ACKNOWLEDGEMENTS

I would like to take this opportunity to acknowledge those who have helped me along the journey of my thesis. First and foremost, I would like my mother for her constant and invaluable support which always helped me to push through the hurt and achieve all of my goals. Second, I would like to thank my fiancé because without him I would have never had the courage to go back to school. I would like to thank my family for their support with a special thank you to my niece who made me want to strive to be the best karst hydrogeologist she thinks I am. I love you all dearly.

In addition I would like to thank all of my advisors, Eric Peterson, John Kostelnick, and Toby Dogwiler, for their knowledge that they have passed on to me and their help and support.

L.E.H.

CONTENTS

FIGURES

CHAPTER I

INTRODUCTION

Introduction to Karst

Karst is all the surficial and subterranean features that form from dissolved bedrock. The most notable karst features are caves. Cave entrances are found at the surface while the majority of the cave is below the surface. Other karstic features noticeable at the surface are sinkholes and sinking streams. Another subterranean feature is the epikarst, which is the weathered limestone below the regolith or soil interface. Karst forms from the dissolution of bedrock, typically carbonates (specifically limestone and dolomite) by acidic groundwater. The acidity in groundwater is most often from the formation of carbonic acid. The carbonic acid forms when infiltrating water is charged with carbon dioxide in the soil. The carbonic acid will exploit any cracks or fractures within the bedrock and create larger openings. Fractures and bedding planes become the favorable routes for dissolution in cave formation. This is a slow process that can take several thousands of years to form caves from the original cracks within the bedrock (Martin and Gordon 2000). These cracks can be expressed at the surface as lineaments which can aid in the detection of karstic areas.

As mentioned above, karstic terrains contain cavernous areas and can have sinkholes and sinking streams. The sinkholes can be created when a cave or large fracture open collapses due to the heavy overburden above the opening in the subsurface. They can also form due to solutional or subsidence-driven development. Sinkholes have been widely studied as a means to locate karst. Sinkholes can be very large features and are easily located on a map; therefore,

they are beneficial in predicting errors in a DEM when using computer software to map karst areas (Angel et al. in 2004).

The epikarst and cave channels (conduits) are the main components of a karst system. The epikarst is the uppermost portion of a karst system and is in the vadose zone; therefore, it is in contact with the soils and the atmosphere. Cave channels can be in the phreatic zone or in the vadose zone. Both the epikarst and the channels provide pathways for the rapid transmission of groundwater flow.

Flow within karstic terrains is more complicated than porous media groundwater flow. Porous media groundwater flow involves mainly laminar flow through the pore spaces within the soil and sediments. In karstic terrains, groundwater does flow through pore spaces (matrix flow) but flows turbulently through cracks, fractures, and cavities (conduit or quick flow). The difference between the conduits and the rock matrix is that the matrix is the main location for storage and the conduits are the main avenues of transport. However, the caves within a karstic aquifer can either be dry or wet. Dry (vadose) caves are primarily above the water table but can be included in the water table during rainstorm events. Wet (phreatic) caves are at or below the water table, resulting in full or partially filled conduits. During rainstorm events, partially filled channels and cracks can become flooded. During a flooded stage in a karstic aquifer, the flow condition changes. The generally turbulent nature of flow can become

laminar in the center of the channel while remaining turbulent at the edges (Annable and Sudicky 1999).

According to Mahler et al. (1999), the highly localized, heterogeneous, and anisotropic permeability of karst systems combined with turbulent flow make karst systems difficult to model. On a small-scale, karstic aquifers can behave like porous media, have laminar flow, and have predictable flow patterns. However, on larger scales the confidence level for predicting groundwater flow through the aquifer dramatically decreases as the number of flow pathways increases due to conduit branching (Annable and Sudicky 1999).

Flow through a karst system is not always subterranean; it can also be surficial. When a stream starts at the surface, eventually goes underground, and resurfaces along the flow path it is deemed a sinking stream. These streams are characteristic of karst terrains and can augment karstification of the area. This type of stream complicates the modeling of a stream network because most models assume the flow of the streams is at the surface.

Another complication to karstic systems involves the intricacies and advanced development of the system. A karst system can develop in levels due to fluxuations in the water table level or due to base level changes from an incising river (Palmer 1987). The lower levels of caves could be forming at the same time as the higher caves, but the lower caves would be forming due to phreatic processes and not changes in base level. Elevations of caves are used to help identify the levels within a karst system.

In northeastern Kentucky, the ancient stream network was part of the Teays River drainage system. In the Pleistocene, glaciations dammed the Teays River creating lakes where once flowing rivers were located. As the glaciers retreated, new drainage networks formed, including the Ohio River System (Janssen, 1953). In addition to the Pleistocene glaciations, this area responded to sea level rises and falls. At higher water levels where the water table is relatively stable, multiple caves will form. During regressions, ocean levels fall creating a lower base level and thus causing rivers to incise. A river will down cut through rock to reach base level, with the ultimate goal of reaching sea level to reduce the amount of energy in the system. Multiple levels in a cave system are created when a river is incising (Anthony and Granger 2004; Granger et al. 2001; Palmer 1987).

In the northeastern Kentucky area, as Tygarts Creek incised through the Mississippian limestone formations, a karst area began to form (Jansen, 1953). Over periods of transgression and regressions the development levels within the caves became prominent (Tierney, 1985). The caves within the Cave Branch system are in the Ste. Genevieve Limestone and the St Louis Limestone. Caves along Horn Hollow are in the Ste. Genevieve Limestone. Most other caves within the CCSRP are contained within the Upper Member Limestone of the Newman Formation (Hobbs and Pender, 1985). The Tygarts Creek flows to the northeast to the Ohio River.

Scientific Background

In a Geographic Information System (GIS), Digital Elevation Models (DEM) and Digital Terrain Models (DTM) can be used to calculate and represent topographic features (Lo and Yeung, 2006). For example, Yilmaz (2006) used DEMs along with raster spatial analysis in a GIS to model karst depressions. Gao et al. (2006) developed a karst feature database that assists in the analysis and management of geologic and hydrologic datasets at both the regional and local scales.

In Utah, McNeil et al. (2002) used GIS applications at Timpanogos Cave National Monument. A high resolution DTM of 2m was created from digitized 10 foot contours from hard-copy 1inch = 100ft scale maps. The DTM has been used for many applications, such as a creation of a virtual field trip through the cave trails and a rock fall hazard model. The rock hazard model was delineated from a DTM to account for slope and added to a vegetation map to account for friction on the slopes. In addition, the park management uses GIS to manage the natural resources and as a means to create and store databases of the park.

Ohms and Reece (2002) studied Wind and Jewel caves of South Dakota and used GIS to help manage the datasets that are vast due to some $21{,}000^{+}$ cave stations that are continuously collecting data such as elevation, cave location, speleothems, etc. However, the data collected are 2D, and interpolating the data to the third dimension was extremely time consuming. The application of GIS serves as a link between the databases and the surface features.

At Jewel Cave, the data have been used to find locations of toxic weeds close to the cave. Then the depths to the caves below these weeds were calculated to evaluate their proximity to drainages and infiltration zones. The results from this analysis helped management make decisions about the use of herbicides to treat the weeds, while preserving the cave environment by limiting risks of contamination via the surface.

At Wind Cave, management used GIS to understand the relationship between park's the parking lot and the cave. The GIS was utilized to analyze the distance between the cave and the parking lot, which helps delineate the overburden on the cave. The analysis and the nature of the cave/parking lot relationship have assisted in plans to remodel the parking lot at the Wind Cave Visitor Center. The new parking lot will include a runoff treatment system.

Angel et al. (2004) used GIS software to obtain a sinkhole count and examine the potential errors, or miscalculation of the sinkhole count that resulted from using GIS. Sinkholes were counted by hand by interpreting contours on USGS quadrangle maps. Sinkholes were also counted using GIS by adding Digital Line Graph (DLG) hypsography and hydrography data layers and an Illinois Public Land Survey (PLSS) data layer. The results of the study concluded that the difference in the sinkhole count derived manually and from GIS was negligible and therefore the GIS method was accurate enough to use as a way of counting the sinkholes within the given region of study. In addition using GIS was a time saving method over the hand count method.

Florea (2005) used GIS as a means to correlate the sinkholes with the underlying geology. Maps of Kentucky were digitized with GIS software and then geology layers from the Kentucky Geological Survey (KGS) were added resulting in a map showing the correlation of the sinkholes to the karstified bedrock below. The sinkholes were used to aid in the discovery of more faults and fractures below the surface. This study was done to enhance the Karst database of Kentucky. The KGS maintains the karst state-wide database for Kentucky. This database is used to aid in the identification of unknown karstified areas and assist with the planning and zoning for Kentucky.

Seale et al (2008) looked at new methods to help find and map sinkholes in Pinellas County, FL, utilizing a newer remote sensing technique called airborne laser swath mapping (ALSM). From the ALSM several points (25,000 measurements/second) were collected. In the study, they obtained more than a billion elevation points. From those points they created a DEM to help locate sinks.

Other researchers use GIS for hydrologic modeling to delineate stream networks and watersheds for their research areas in karst environments. Glennon and Groves (2002), used watershed modeling to identify “key locations” that affect the drainage system within the Mammoth Cave Watershed and ultimately to map out the watershed. Choi and Engel (2003) also used watershed delineation modeling to set up an interactive watershed database of

Indiana on the internet for the public to use. Erturk et al. (2006) used watershed modeling system to help manage water resources in Turkey.

Sahoo et al (2000) studied faults in the northwest Himalayas. They used satellite imagery from IRS-1B LISS-I to aid in the detection of faults and drainage patterns. In order to detect lineaments they found that the best band to use was band 4 (near-infrared band). They filtered band 4 with 3x3 filters in the horizontal, vertical and two in the diagonal direction to enhance edges. The lineaments detected were compared to ancillary data (topographic maps) to rule out roads and canals. The remaining features (which were dark lines) were digitized and therefore classified as a lineament. The major faults were detected by visual interpretation of the false color composite image. The lineaments were then compared to the location of rivers and they found that the rivers are controlled by the faults and joints in the area. In a related study, Litwin and Andreychouk (2008) used monochromatic stereo pairs of aerial photos that were colored for elaboration to acquire characteristics of high-mountain karst. They also used the photos as a means or defining the vegetation cover and detected lineaments.

Ali and Pirasteh (2004) studied the Zagros Structural Belt in southwest Iran using Landsat Enhanced Thematic Mapper (ETM+) images to make structural interpretations of folds and faults. The lineament detection was based on vegetation linearity, tonal changes, drainage patterns, topographic breaks, tectonic landforms, and landscapes and discontinuities in the same lithology.

Saraf et al (2000) used remotely sensed data to delineate springs and watersheds and study the discharge patterns. Using ancillary data of a Survey of India (SOI) topographic map and land use maps from 1981 along with the remotely sensed images from IRS 1C LISS-III from 1997, they generated land use maps and looked at the impacts of land use changes on spring locations and discharge points. Being able to delineate a watershed and drainage patterns is important to geologists and hydrogeologists because knowledge of the location of a watershed may aid in the understanding of the how water flows through the given area. In karstic area, the information can aid in the understanding of the processes that formed subterranean and surficial karst features. Understanding the processes and behaviors of karst landscapes and their subterranean stream networks will help with better utilization and management of the Earth's natural resources (Glennon and Groves 2002).

Yilmaz (2007) studied the probability of collapse hazard in karst terrains in Turkey using remotely sensed data. Several factors were looked at to determine if an area is susceptible to collapse, such as lithology, the drainage system, structural lineaments, morphology, springs and vegetation cover. They first located depressions, sinks, and lineaments using aerial photos, satellite images, and field work. Satellite images from Landsat Thematic Mapper (TM) were used to calculate a Normalized Difference Vegetation Index (NDVI) from the red and near-infrared bands. A DEM, derived from topographic maps, was used to calculate slope and elevations. They found that areas with a slope of less than

ten degrees, a lithology of gypsum, close proximity to lineaments (folds, faults, and roads), close proximity to rivers, and an NDVI of less than 0.1 (barren rock) on a scale of 0-1 are the most susceptible to collapse. This study is now used to assist in collapse hazard management and land use planning.

In Vietnam, a project has been on going to find a sustainable water source in the northwest. The area is karstified and not understood very well. In order to gain knowledge of the area, Hung and Dihn (2002) used remote sensing and applications of GIS to help build a cave database. Lineaments were digitized and compared to aerial photos to help discern geologic lineaments from roads in the area. They found areas with a higher density of lineaments indicated a high intensity of deformation in the area. In addition they found that these lineaments followed the same trend as the major fractures and faults in the area. In the cave analysis, a distance function was used to calculate the distance between the cave and the nearest cave. Then a buffer was set up to make sure the entire cave was covered. A comparison of the caves to the lineaments was made. They found that the caves followed the same trend as the lineaments and most of the caves were within meters of the lineaments. Thus they surmised that the caves formed along joints and fractures in this area. Because of the study the Vietnamese have a way of predicting where caves will be based on the lineament density in a fractured zone.

Purpose/Significance

GIS is widely used in a variety of disciplines to assist in the understanding of observed conditions through spatial modeling. One such discipline is geology, including the analysis of karstified bedrock terrain. Modeling the physical domain of karst features is difficult to due to the highly irregular fractures that don't always follow a distinct pattern. It is also difficult to model chemically, in terms of groundwater flow, due to the irregular flow patterns and the turbulent flow through the open channels. GIS is becoming increasingly used by state agencies to set up databases and help model karstic terrains (Florea et al., 2002). GIS provides several potential benefits such as the ability to store a large amount of information and display that information visually, either in 2D or 3D.

The objective of this research was to use GIS to create a conceptual model that will help develop a better understanding of the karst within Carter Caves State Park and Resort (CCSRP). The first objective was to create a GIS database for the CCSRP. The database is very important because ISU, Winona State University (WSU), and Wittenberg University (WU) will ultimately use the database for further research of the cave system. The database includes information about cave locations and elevations as well as topographic maps. (As a side note, the information in the database is kept on a secured server within the Institute for Geospatial Analysis and Mapping (GEOMAP) at ISU in order to protect the caves and their locations within the park. Therefore cave locations in this thesis will not be discussed and only approximate locations will

be shown on maps.) Next, while creating the conceptual model, the GIS will aid in mapping out the cave entrances to answer the question of whether there are multiple levels within this system. In addition, a method utilizing DEMs and remotely sensed data will be used to help detect sinkholes and lineaments in the CCSRP. From the data (elevation, sinkhole locations, cave locations, etc) in the karst database, a model of the karst terrain can be created and be used to further the karst research. Lastly, GIS will be used in conjunction with topographic maps to generate data about stream networks in the park and map out and model the stream network within the CCSRP. The area within the CCSRP, in Carter County, Kentucky, is karstified, containing caves, pits, sinkholes, and sinking streams. Therefore, the complete stream network is not present at the surface, but instead a fragmented river system. Due to the presence of these fragmented rivers, an understanding of the stream network in the area needs to be further researched.

CHAPTER II

BACKGROUND AND METHODOLOGY

Geologic Setting and Site Description

According to Florea (2005), roughly 55% of Kentucky is underlain by karstified limestone, and sinkholes cover 4% of the regional area. The Carter Caves State Resort and Park (CCSRP) is located in the northeastern portion of Kentucky within Carter County (Figure 1) and is highly karstified.

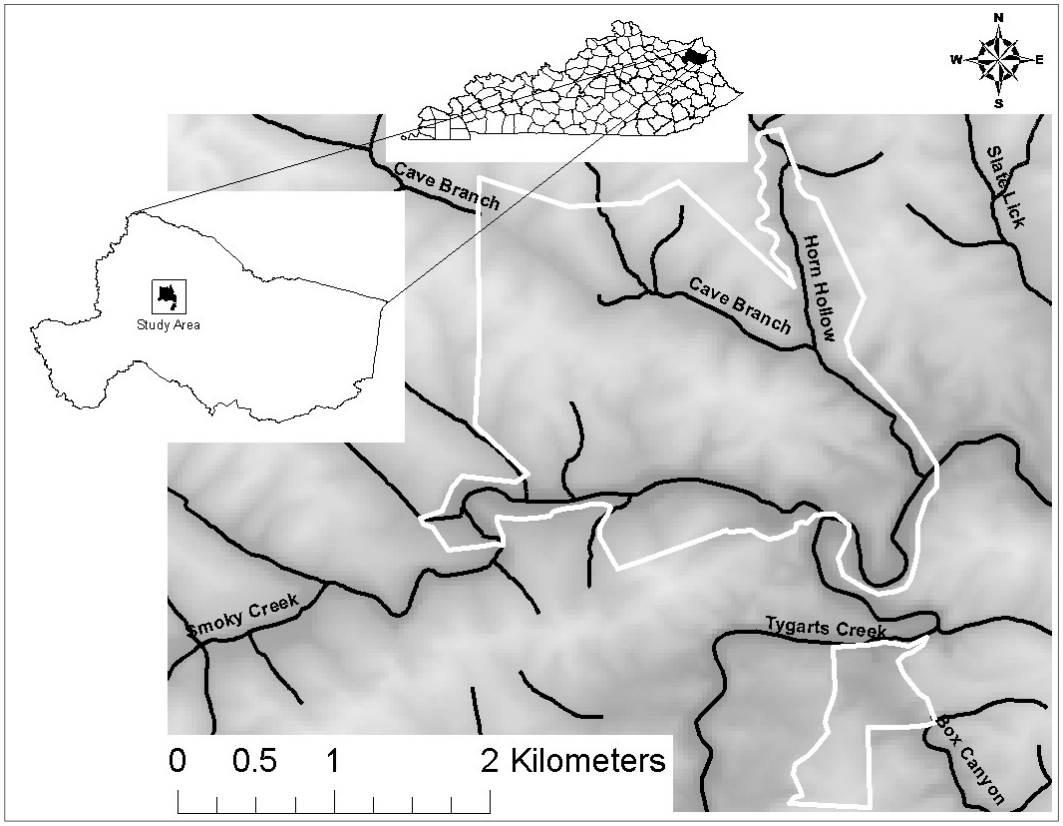

Figure 1. Location of Carter Caves State Resort Park. The park is outlined in white and the rivers are in black. Park boundary and Rivers data obtained from Kentucky Geologic Survey (2008) and DEM were obtained from the United States Geologic Survey (1999).

In a 40-kilometer radius of Carter Caves there may be as many as 200 caves and pits (Tierny, 1985). The karst and cave features are located within Mississippian limestone (Upper Newman Limestone, Ste. Genevieve Limestone and the St Louis Limestone) and capped by Pennsylvanian sandstone (Lee Sandstone). Beneath the limestone is the Borden Formation, resistant layers of shales and siltstones (Figure 2). The Upper Newman Limestone can have a thickness of four to twenty-four meters. The Ste. Genevieve Limestone can be eighteen to thirty-four meters thick. The St Louis Limestone can be up to four and a half meters thick. The Borden Formation can be up to sixty meters thick.

This area has experienced some uplift associated with the Waverly Arch. In general, the beds have a slight dip of 0.3^{o} to 2^{o} to the east-southeast (McGrain, 1966; Engel and Engel, 2009; Woodside, 2008). However, the heavy cross-bedding seen within the Ste. Genevieve Limestone make it difficult to determine an exact dip in the field.

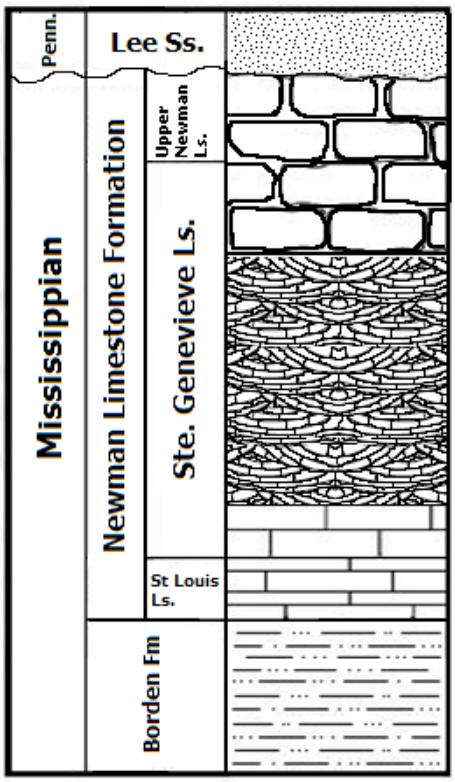

Figure 2. Stratigraphic Column showing the geologic layers seen in the CCSRP. (Created after McGrain, 1966)

The Borden Formation prevents further down cutting and may be the cause of the extensive karst in the area because it is resistant shale. Subsequently, several different caves systems are located within the CCSRP (McGrain, 1966). However, the relationship between the different caves and the levels of the system are not known.

Cave Branch is the main stream in the CCSRP and is a tributary to Tygarts Creek (Hobbs and Pender, 1985). Tygarts Creek is the major stream that flows through this region, and it has contributed to the erosion of the

Mississippian limestone. Other tributaries to the Tygarts Creek that have contributed to the erosion of limestone within the CCSRP are Horn Hollow, Smoky Creek, and Box Canyon. Tygarts Creek flows northeast and is a tributary to the Ohio River. The Tygarts Creek has down cut to the Borden Formation and is no longer an active source of erosion to the limestone in the CCSRP (Tierney, 1985; Engel and Engel, 2009)

Methods and Materials

GIS data (topographic maps, a hydrography layer, a park boundary layer, a DEM, orthophotos of National Agriculture Imagery Program (NAIP) and Digital Orthophoto Quarter Quads (DOQQ), Landsat imagery, and cave locations from the websites of the Kentucky Geological Survey (www.uky.edu/KGS/gis/index.htm) and the United States Geological Survey (seamless.usgs.gov), as well as karst features data, that includes the names of caves, sinks and pits, and their locations, collected by mainly WSU and secondary data set collected by WU were used in the development of this project. ESRI's ArcCatalog was used to build a geodatabase for the collected data. The final database was converted into SDE format so it can be accessible to multiple users.

The DEM used has a 30m by 30m spatial resolution and was created by the USGS in 1999. Vertical accuracy of the DEM was assessed by comparing the DEM value to Ground Control Points (GCP's). The overall accuracy was

described in terms of the root mean square error (RMSE), the National Map Accuracy Standards (NMAS), and in terms of the National Standard for Spatial Data Accuracy (NSSDA). These values for the 1999 DEM's are 3.74, 6.15, and 7.34 respectively. The NMAS value means that 90% of the values were within 6.15m of the GCP value. The NSSDA value means that 95% of the values were within 7.34m of the GCP value.

The KGS GIS stream data was taken from the USGS National Hydrography Dataset (NHD) which was created from 1:24,000 Digital Line Graphs (DLG). The NHD has an accuracy of 98.5%.

Cave levels were based on the elevations of the caves. The karst features location data were imported into ESRI's ArcMap 9.2 based on the latitude and longitude given for each cave. Once in ArcMap, the cave locations file was changed over to a permanent shapefile and re-projected from the North American Datum of 1927 (NAD27) to the North American Datum of 1983 (NAD83), since all the other GIS data collected for this project was in NAD83. Using a query function, the caves were selected in order to remove the pits and sinks forming two files (one of the caves and a second for the pits and sinks). In doing this the results would just focus on the caves. In order to obtain the elevations, for all the caves, a DEM was added. All elevations for each cave were added to the cave location shapefile. The elevations obtain from the DEM were compared to the elevations collected by WSU. From there, a histogram showing the frequency of cave entrances at every meter change in elevation

(based on the ArcGIS algorithm of a Natural Breaks Classifier) was generated to classify the levels within the cave system. The cave levels were delineated based on where there was a high frequency of caves at one elevation with breaks or no cave entrances on both sides. The histogram contains many breaks and several levels could have been classified based upon personal interpretations. The elevations were exported out of ArcGIS into an Excel file for the calculation of basic descriptive statistics such as mode, mean, median, and range.

The cave elevations obtained by using a DEM were compared to the field data collected by WSU. The elevation data collected by WSU were obtained in the field by using a DGPS, topographic maps, an electronic altimeter, and a Kestrel. The data were in UTM and added into ArcGIS and were re-projected into NAD83. Then the DEM was added and the elevations from the DEM were extracted and added to the WSU elevation data file.

In addition to finding the cave entrance elevations, the distance a cave entrance is from a stream was derived. To derive the distance from a stream, first, the stream layer, which was derived from a DEM, and the cave entrances layer were re-projected into Zone 17 UTM to derive distance units in meters. Once in UTM, the stream layer was input into the EUCLIDEAN DISTANCE tool, which is a sub-routine function in ArcGIS. The output is a raster grid that contains the distance from a stream for the entire input area. Then, using the EXTRACTION tool, again a sub routine of ArcGIS, the distance values from the

raster were extracted and added to the cave entrance layer. The data were exported into an Excel file to break the caves into the levels derived.

In order to create a stream network for the CCSRP, GIS data (Topographic maps, the park boundary, a hydrology layer, and a DEM) were added into ArcMap, a program from ERSI's ArcGIS 9.2 software. Using ArcMap a Stream Network Model (Figure 3) was created using Model Builder in ArcMap to delineate the stream network from the DEM.

In the Stream Network Model, the sinks (a term used in GIS to describe a cell with a lower elevation value than the surrounding cells elevation values) in the DEM are filled using the FILL tool. The sinks in the DEM are filled because the water that flows in a sink cannot flow out which creates a problem when calculating the flow direction raster. Therefore sinks are considered as errors in a DEM. (The word sinks written hereafter is only in reference to GIS and is not necessarily a karst feature of a sinkhole.) Once the DEM is filled, a flow direction raster can then be calculated using the FLOW DIRECTION tool. The resulting raster shows the direction in which water flows from cell to cell. From the flow direction raster a flow accumulation raster is created using the FLOW ACCUMULATION tool. The flow accumulation raster shows the number of cells upslope that flow to the same location. Then the CON tool is used to define the stream network. The CON tool uses an expression that sets a threshold. The threshold is the minimum number of cells that must flow into one cell in order for that cell to become part of the stream network. The resulting raster and the flow

direction raster are input into the STREAM LINK tool and a stream network raster is delineated. The stream network raster is then converted into a vector shapefile. In addition to delineating the stream network, the watershed and sub-basins were calculated from the flow direction raster and stream network raster using the WATERSHED tool.

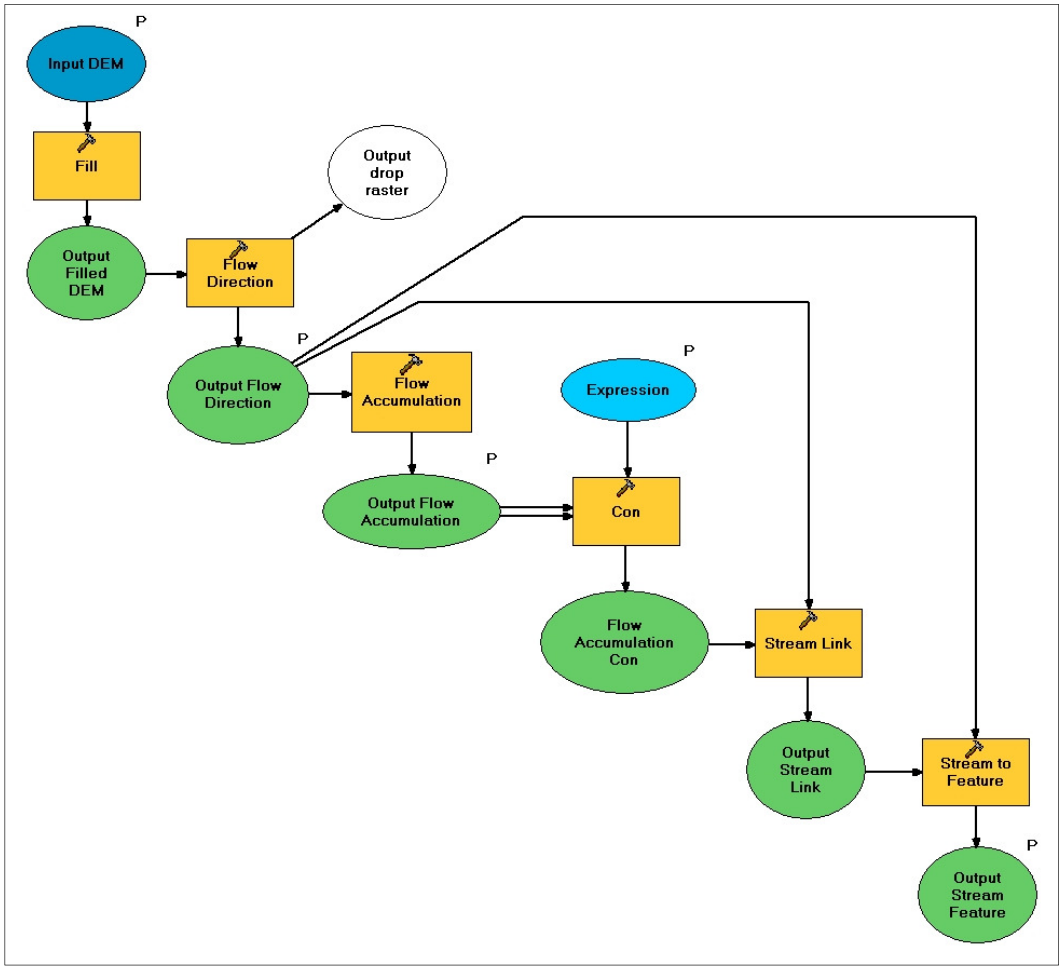

Figure 3. Stream Network Model (The yellow boxes are subroutines from ArcMap, the green ovals are the output layers.)

The model was run three times with different threshold values (10,000 cells, 1,000 cells, and 100 cells). This was done because the threshold number depends on the relief in a given area and the resolution of the DEM. The resulting stream networks were compared to the KGS stream data to calibrate the model in order to access if using GIS is a plausible way of creating a stream network.

A fourth trial of the model was run to see the effects of the FILL tool had on the development of a stream network. In this trial the sinks were identified first using the SINKS tool. The SINKS tool located areas in the DEM where a low point is surrounded by higher elevations. These sinks located are not necessarily sinkhole features that a karstic terrain may exhibit. In karst sinkholes can be shown on a DEM and are not considered errors. Therefore a fourth trial was run to see if the sinks in the DEM would affect the outcome of the stream delineation. In this trial, the previous stream network with a threshold of 100 cells was compared to a stream network created from not using the FILL tool at threshold of 100 cells and to a stream network where the sinks were filled but the sinkholes were not filled. In order to create a DEM where the sinkholes were not filled but the sinks were filled, the sinkhole layers were overlaid onto the sinks layer. This was done by creating a buffer around the sinkhole points and converting them into raster format because the sinks layer was in raster format. If a sinkhole overlaid a sink a conditional expression was created such that where sinkholes were the original DEM values was kept, but where there was a

sink the filled DEM value was taken. The newly created DEM was then run through the stream network model starting at the flow direction step.

Remotely sensed data were used in conjunction with the DEM and topographic maps to locate sinks in the area. The images from Landsat7, DOQQ and NAIP were added into Leica Geosystems ERDAS IMAGINE 9.2. The 1m resolution DOQQ images were mosaicked together and then resolution merged with the 4 band resolution Landsat7 image using the MOSAIC and MERGE tools. From the composite image the fourth color band (the Near Infrared band) was isolated and filtered with a Laplacian filter. Once the filter was complete, the image was brought into ArcGIS to digitize the sinkholes and lineaments. Sinkholes were identified based on where there was a dark spot on the image that corresponded to a topographic low on the topographic map.

In order to detect the lineaments the same Laplacian filtered NIR image was used. The Laplacian filter makes any lineaments in the given image show more prominently. Therefore, a roads layer was added into ArcMap to distinguish them from geologic lineaments. Once the roads were excluded, the geologic lineaments could then be digitized. These geologic lineaments were digitized to see if they and cave locations would follow the same trend.

CHAPTER III

RESULTS AND DISCUSSION

The GIS database

The created database was called CCSRP and will be placed on a secured server in the ISU GEOMAP lab. The only persons that will be able to access the database will be my advisors (Dr. Eric Peterson, Dr John Kostelnick, and Dr. Toby Dogwiler). They will determine who will be granted access. Again, this was done to insure the protection of the location of the caves and to help preserve the caves within the CCSRP. The resulting geodatabase contains the following information:

1. The WSU cave entrance names, elevations and locations by
    a. Latitude and longitude
    b. Topographic map
2. WSU elevation field data with DEM elevations
3. The park boundary shapefile
4. Carter County shapefile
5. Six topographic maps that encompass the CCSRP
6. DEM
7. A rivers within Carter County shapefile
8. The distance cave entrances are from a stream shapefile
9. A geology of Kentucky shapefile
10. The karst areas in Carter County shapefile and
11. Overlapping caves shapefile.
12. Stream network data at all thresholds(10,000; 1,000; and 100) including

a. Flow direction
b. Flow accumulation
c. Watersheds
d. Stream networks
e. Sinks in the DEM raster

13. Remotely sensed data of
    a. DOQQ
    b. Landsat7
    c. NAIP

The database is in two formats (DBF and SDE).

Cave Levels

Two hundred nine cave entrances and pits were plotted in ArcGIS 9.2. Most of them plot near the Tygarts Creek, Cave Branch, Horn Hollow or Smokey Creek (Figure 4). They are found near rivers because the incising rivers exposed the passages, thus, creating the entrances. A shapefile of the overlapping caves was created and added to the database in order to aid in the future research.

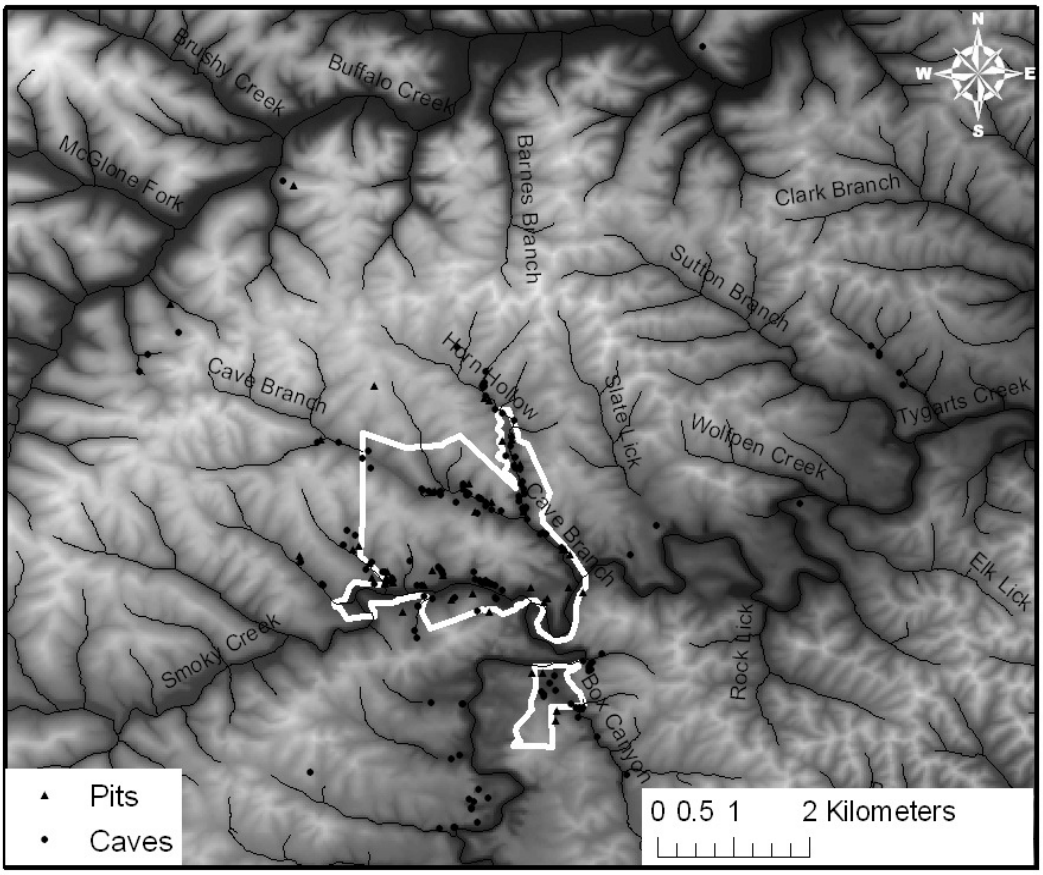

Figure 4. Locations of the caves and pits in and around CCSRP.

From the two hundred nine cave entrances and pits, one hundred sixty were caves and cave entrances and forty nine were pits. Three of the one hundred sixty cave entrances were excluded because they overlapped another cave entrance. (Most likely these are the same cave entrance but they are called by two different names.) The forty nine pits were excluded from the classification of levels. Although pits are a karstic expression, they are vertical features and this project only deals with karst features formed in the horizontal and thus they were excluded.

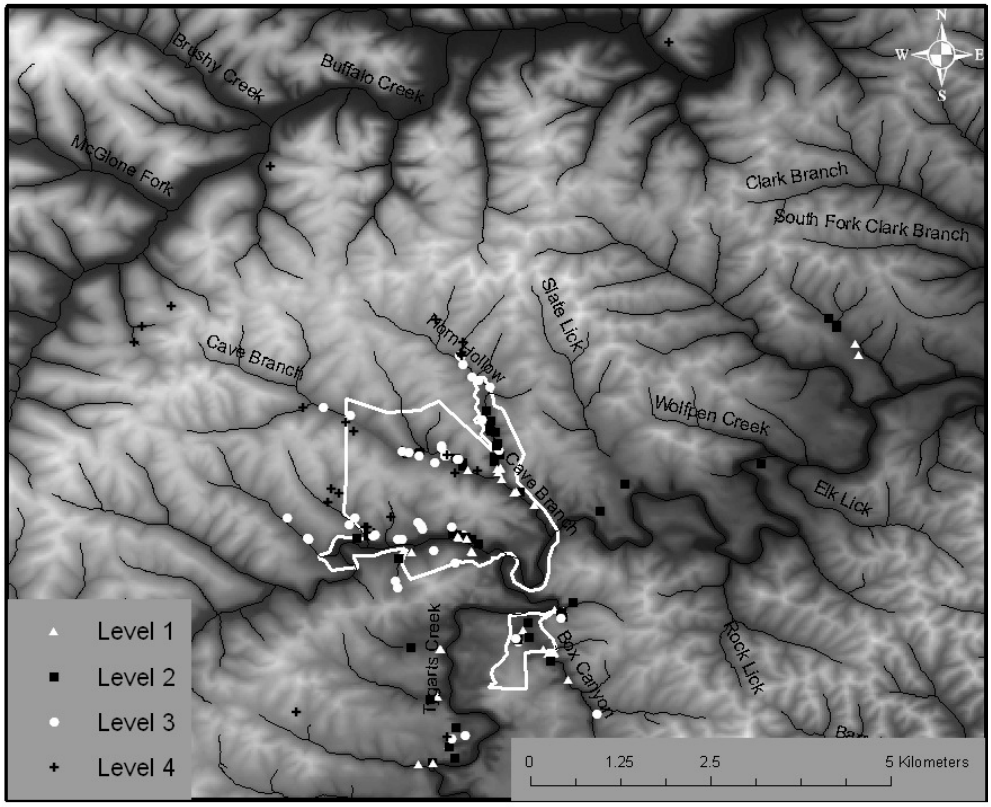

Figure 5. Location of the cave entrances and their elevations. Level 1 is at the lowest elevations and Level 4 is at the highest elevations.

The cave elevations were plotted in ArcGIS to see if there was a distinct pattern to the locations (Figure 5). In general, the highest cave entrance elevations were furthest from the rivers and the lower cave entrances were still in contact with the rivers. The furthest caves from the river should be dry caves and no longer be actively forming due to the disconnection from the water table. The lower cave entrances in contact with the water table will still be actively forming large caves due to the geology.

Tygarts Creek has incised down to the Borden Formation which consists of resistant shales and prevents further down cutting, and thus, is preventing new levels within the cave system from forming. Cave Branch, Horn Hollow, and Smoky Creek will down cut or incise through the limestones until they reach the base level of Tygarts Creek and could possibly have active cave systems.

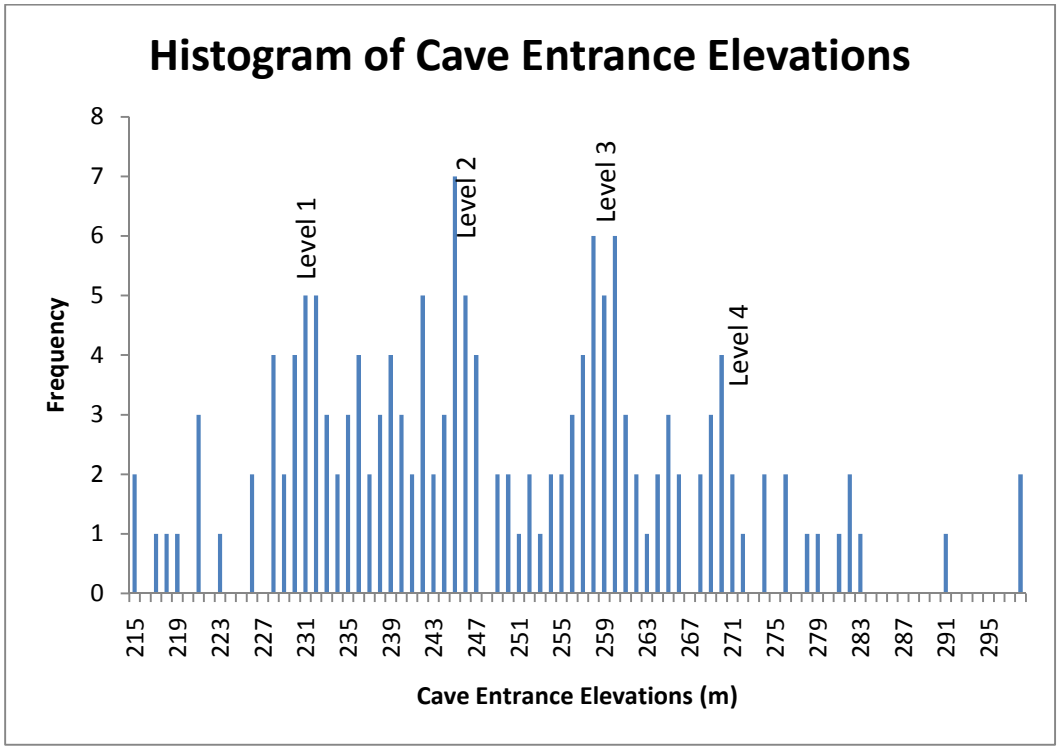

Figure 6. Histogram of all the cave entrance elevations from DEM data.

Within the CCSRP a total for four levels were observed (Figure 6). These levels were classified based on where there was a high frequency in the number of cave entrances at a given elevation. Level breaks were based on gaps in the elevations of the entrances (Individual elevations are listed in Appendix A). The

histogram contains many breaks and several levels could have been classified based upon personal interpretations.

Large breaks after a high frequency in cave entrances in the histogram were used to surmise the distinct levels. The levels shown in Figure 6 (represented by the mean value for each level) were at 231 to 232m (Level 1 - L1), 245m (Level 2 - L2), 258m to 260m (Level 3 - L3), and a minor level 270m (Level 4 - L4). At Mammoth Caves (Palmer, 1987) there are only four major levels (at 152m, 168m, 180m and 210) with a few minor levels. In 2001, Granger et al described four levels (at 150m, 167m, 170 to 180m, and 200m) for Mammoth Caves. The levels at Mammoth Caves are lower in elevation than those found within the CCSRP. Like the CCSRP, the majority of the caves are found in the Ste. Genevieve Limestone. These levels coincide well with the finding for the CCSRP, in that they have the same number of levels, which one would expect because the caves are close geographically. These systems are geographically close and therefore should have a close connection to history and development of levels within their respective cave systems because they are affected by the same base flow of the Ohio River. Most of the caves are near the streams of Cave Branch, Horn Hollow, Smoky Creek, and Box Canyon (which is just outside the CCSRP to the southeast).

In addition to the elevations, distances from the caves to the closest river were derived (individual distances are listed in Appendix B with a box plot). On average, the cave entrances in L4 were 72m away from streams which is the

furthest from streams and the cave entrances in L1 were 24m away from streams which are the closest to streams. This is to be expected because as a river incises the valley gets wider and the higher elevations migrate further from the stream.

Level 1 (L1)

Thirty six of the cave entrances are in L1, which makes up 23% of the total cave entrances surveyed. The highest frequency of the cave entrances is found around 231m to 232m in this level. The mode is 231m, the mean is 228 and median elevation is 230m. The level encompasses the elevations of 215m to 234m. This level contains gaps in elevation at 216m, 220m, 222m and at 227m. L1 cave entrances are on average a distance of 24m from a stream. They range from 0 to 54m from a stream.

L1 cave entrances and caves are found in the in the lower to mid-reaches of Cave Branch, Horn Hollow, Smoky Creek, and Box Canyon. Laurel Cave is in this level (entrances at 226m, 230m, and 231m) is located within the Ste. Genevieve Limestone (McGrain 1966; Engel 1999). Another cave entrance in this level is the Cool James Cave-Middle Entrance (elevation 232m), which is known to be in the St. Louis Limestone (Engel and Engel, 2009). Lake Cave (elevation 228) is another cave entrance in L1 and is within the Ste. Genevieve Limestone (Engel and Engel, 2009). Therefore, the caves in L1 were formed in the Ste. Genevieve and St Louis Limestones.

Level 2 (L2)

Forty-seven of the cave entrances are in L2, which makes up 30% of the total caves surveyed. The highest frequency of the cave entrances is found around 245m in this level which is the mode number. The mean and median elevations are 242m. The level encompasses the elevations of 235m to 247m. This level contains no gaps in elevation. L2 cave entrances are on average a distance of thirty-three meters from a stream. They range from 0 to 184m from a stream.

These caves are found in the mid to upper reaches of Cave Branch, Horn Hollow, Smoky Creek, and Box Canyon. This level contains the entrances to the Horn Hollow cave system (entrances at 239m, 242m, and 245m) which is known to be contained within the Ste. Genevieve Limestone (Hobbs, 1985; Woodside 2008). Another cave entrance in L2 is the upper entrance to the Cool James Cave (elevation 242m) which is within the Ste. Genevieve Limestone (Engel and Engel, 2009). Therefore, the cave entrances in L2 formed within the Ste Genevieve Limestone.

Level 3 (L3)

Forty-nine of the cave entrances are in L3 which makes up 31% of the total caves surveyed. The highest frequency of the cave entrances is found around 258m to 260m in this level. The mean elevation is 261m and median elevation is 260m. The level encompasses the elevations of 249m to 266m.

This level contains no gaps in elevation. L3 cave entrances are on average a distance of forty-one meters from a stream. They range from 0 to 157m from a stream.

These caves are found in the upper reaches of Cave Branch, Horn Hollow, and Smoky Creek valleys. This level contains the entrances Saltpetre Cave (elevation 261m) which are formed in the Ste Genevieve and the Upper Newman Limestone (McGrain, 1966). Another cave entrance in L3 is Rat Cave (elevation 260m) which is contained in the Ste. Genevieve Limestone (Engel 1999). Therefore, L3 cave entrances were formed in the Ste. Genevieve and Upper Newman Limestone.

Level (L4)

Twenty five of the cave entrances are in L4, which makes up 16% of the total caves surveyed. The highest frequency of the cave entrances is found around 270m in this level which is the mode number. The mean elevation is at 276m and median elevation is at 274m. The level encompasses the elevations of 268m to 298m. This level contains many gaps in elevation at 273m, 275m, 277m, 280m, 284m to 290m, and at 292m to 297m. L4 cave entrances are on average a distance of seventy-two meters from a stream. They range from 0 to 210m from a stream. These cave entrances are generally the furthest from rivers.

These caves are found just outside the CCSRP. This level contains the entrance of X Cave (elevation 271m) which are formed in the Ste Genevieve and

the Upper Newman Limestone (McGrain, 1966). L4 also contains Coon in the Crack Cave Entrances I and II (elevations at 268m and 278 respectively), which are both within the Ste. Genevieve Limestone (Engel and Engel, 2009). The caves in L4 are most likely contained with the Ste. Genevieve and Upper Newman Limestones.

WSU Elevation Data

The data collected by WSU was added into ArcGIS to obtain the elevation data from a DEM and compare it to the collected field elevation data. The WSU field data is more accurate than the DEM elevations therefore the two were compared to see how much error in elevation is inherent in the 30m by 30m DEM. The data comparison can be found in Appendix A. The root mean squared error (RMSE) was 5.31 between the field elevation data and the DEM elevations. This number is only slightly higher than the RMSE (3.74) of the DEM; therefore, I would surmise that a DEM is a plausible way of obtaining elevation data.

The cave entrance data from WSU fits in between L1 and L3. In L1 the mode elevation was at 232m and the data from WSU (Figure 7) shows a peak number of entrances at 233m. In L2 and in L3 the modes were at 242m and 258m to 260m respectively. The WSU histogram shows high frequency of caves entrances at 240m to 241m and 258m which coincide well with the DEM cave entrance data. The WSU data was taken along Horn Hollow and Cave Branch.

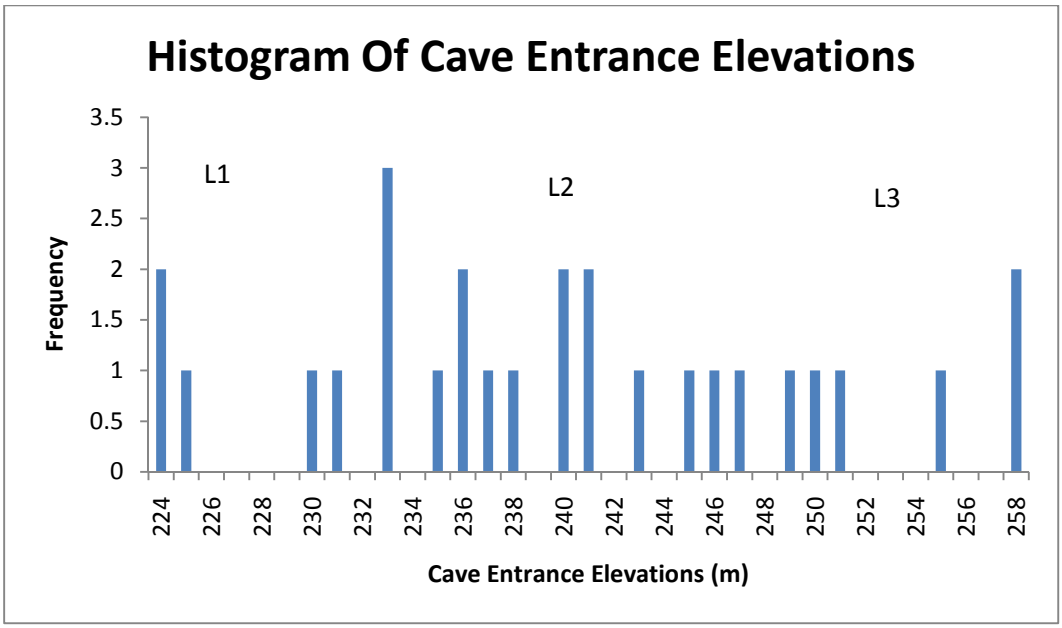

Figure 7. Histogram of the cave entrance elevations from WSU data.

Stream and Watershed Delineation

A karst area naturally has sinkholes, which are problematic for GIS software when determining flow direction. Glennon and Groves (2002) and Wang and Liu (2006) found that not filling the sinks within a DEM of a karst area creates thousands of disconnected streams. Therefore in order to create a stream network, the sinks must be filled and it is crucial to discern the sinks from actual sinkholes to obtain an appropriate model. Three maps (Figure 8) were generated from the Stream Network Model. The resulting stream networks were visually compared to the stream data layer from the KGS GIS database by overlaying them.

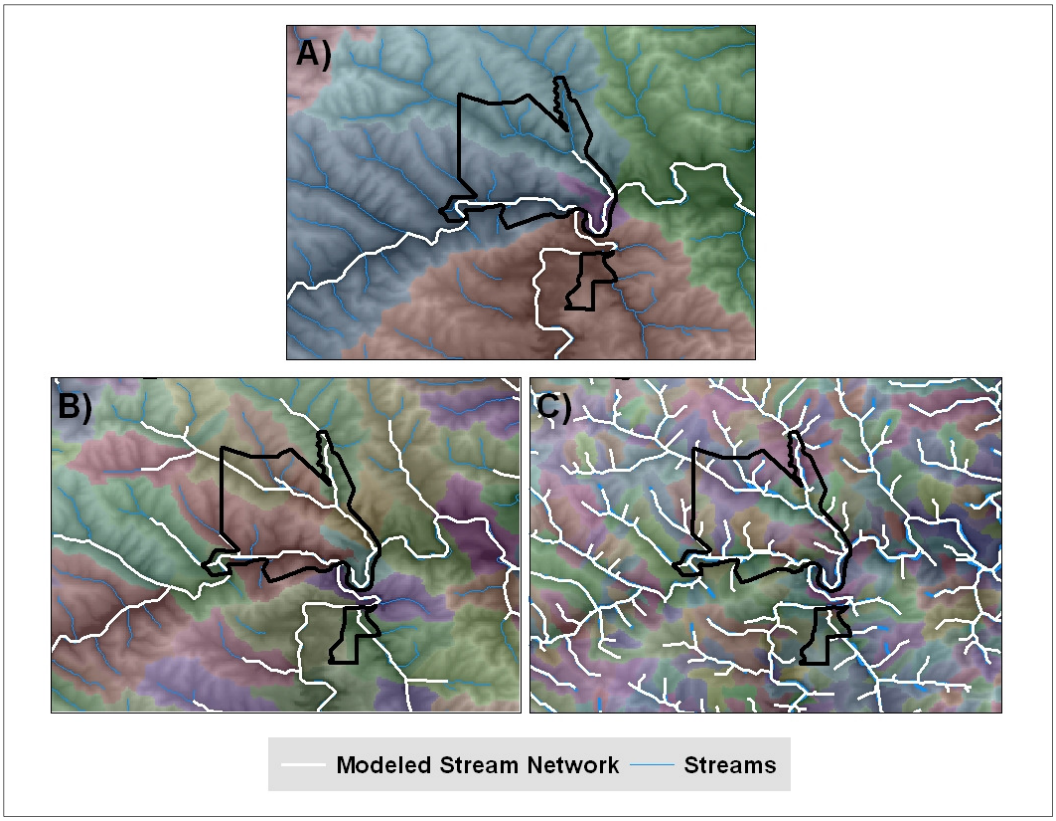

Figure 8. Modeled stream networks A) threshold = 10,000 cells, B) threshold = 1,000 cells, and C) threshold = 100 cells.

When the threshold was set to 10,000 cells, the resulting map has few streams and large watershed areas (Figure 8A). The model seems to underestimate the amount of streams in the area as a vast majority of streams can still be seen. When the threshold was set to 1,000 cells, the resulting map has more streams and more watershed areas (Figure 8B) than the first trial. However, it still slightly underestimates the stream network. When the threshold was set to 100 cells, the resulting map has many streams and small watershed areas (Figure 8C). This was the trial that was the closest to modeling the real life

situation of the streams. The results correlate to what Jenson and Domingue (1988) found which states that as the threshold increase so will the drainage area. Recalling that a stream flows to reduce the potential energy or flows to the path of least resistance and that the GIS model is a surficial model, the stream networks may indicate the historical flow path. If this is the case the sinks identified and filled in the DEM may point to geomorphic or hydrogeologic factors that affected the flow pattern. Therefore the fourth simulation was conducted. Figure 9 shows the locations of sinks within the DEM. Notably the sinks are located where the streams are. Overlaying the sinkholes layer on the sinks layer shows that many of the sinks are actually where sinkholes are and therefore should not be filled.

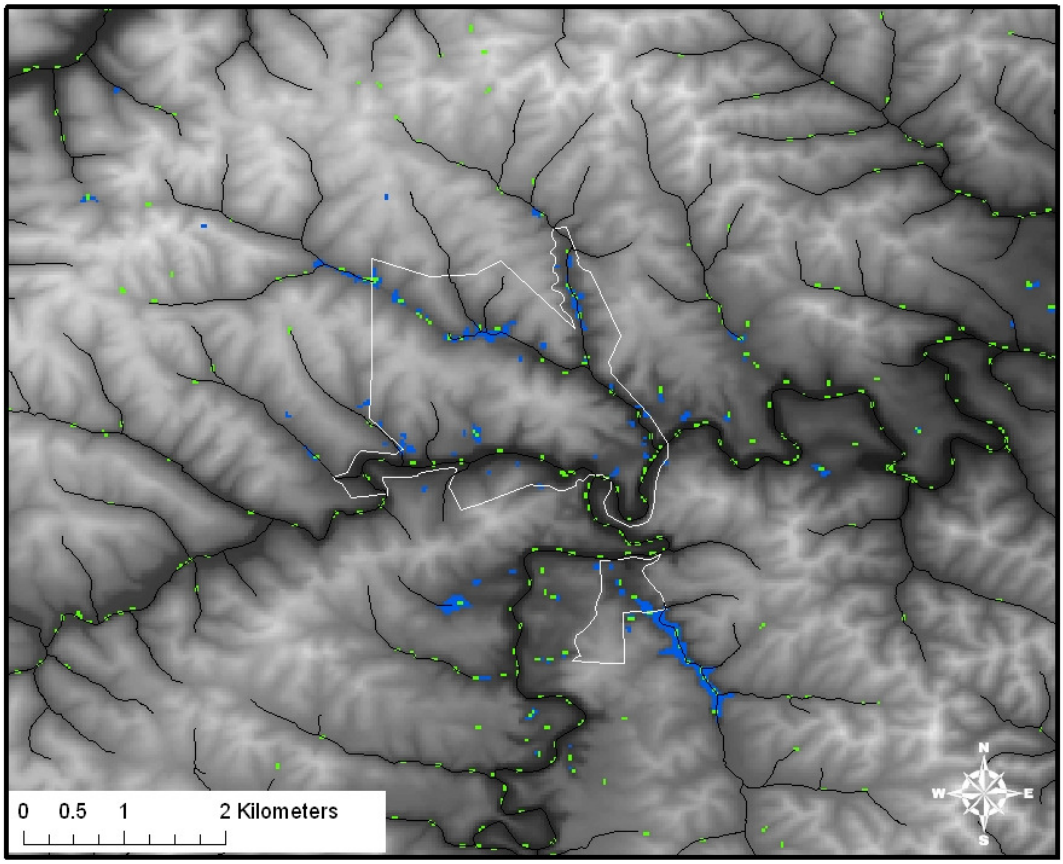

Figure 9. Location of Sinks within the DEM. (Sinks are the green dots and sinkholes are the blue areas)

Once the simulation model was run without filling the sinks a disjointed or fragmented pattern occurred. (Figure 10) The streams weren't connected and created many watersheds but in some areas (near Tygarts Creek) no watershed was delineated.

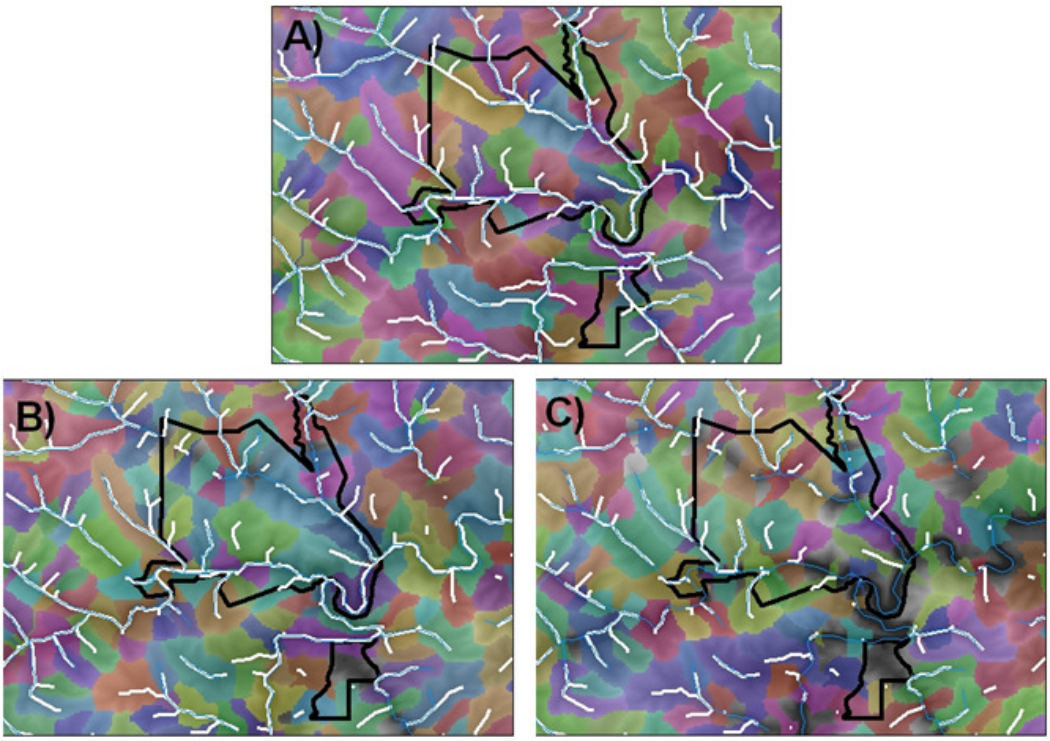

Figure 10. Filled and Unfilled Sinks Stream Network Comparison at a threshold of 100. A) Shows the model with filled sinks. B) Shows the model with unfilled sinkholes and filled sinks. C) Shows the model with unfilled sinks.

Sinks and Lineament Detections

Sinks and Lineament detection were done to see if there was an overall trend as to where the caves were occurring within the CCSRP.

Lineaments

Lineaments were detected in the CCSRP area by running a Laplacian filter on the NIR band of a Landsat7 image that was merged with a DOQQ (Figure 11). In order to only digitize the geological lineaments a roads layer was

added. However, roads can be easily deciphered from geological lineaments because in the NIR band roads appear white to light grey whereas geological lineaments appear to be dark grey. The lineaments detected trended on a northwest to southeast pattern in the northern part of the CCSRP. The fractures are parallel to the rivers and thus are on the same trend as the cave entrances. In the southern part of the CCSRP the lineaments trended on an almost southwest to northeast pattern. This trend is perpendicular to the trend of the cave entrances. Engel and Engel, 2009, studied the orientation of fractures and joints and cave passages thru the use of rose diagrams and found that greater than 77% of the cave passages were within one standard deviation of the NW to SE pattern. They found that the Ste Genevieve and the St Louis Limestones have a mean vector of 304.4^{o} and 317^{o}, respectively.

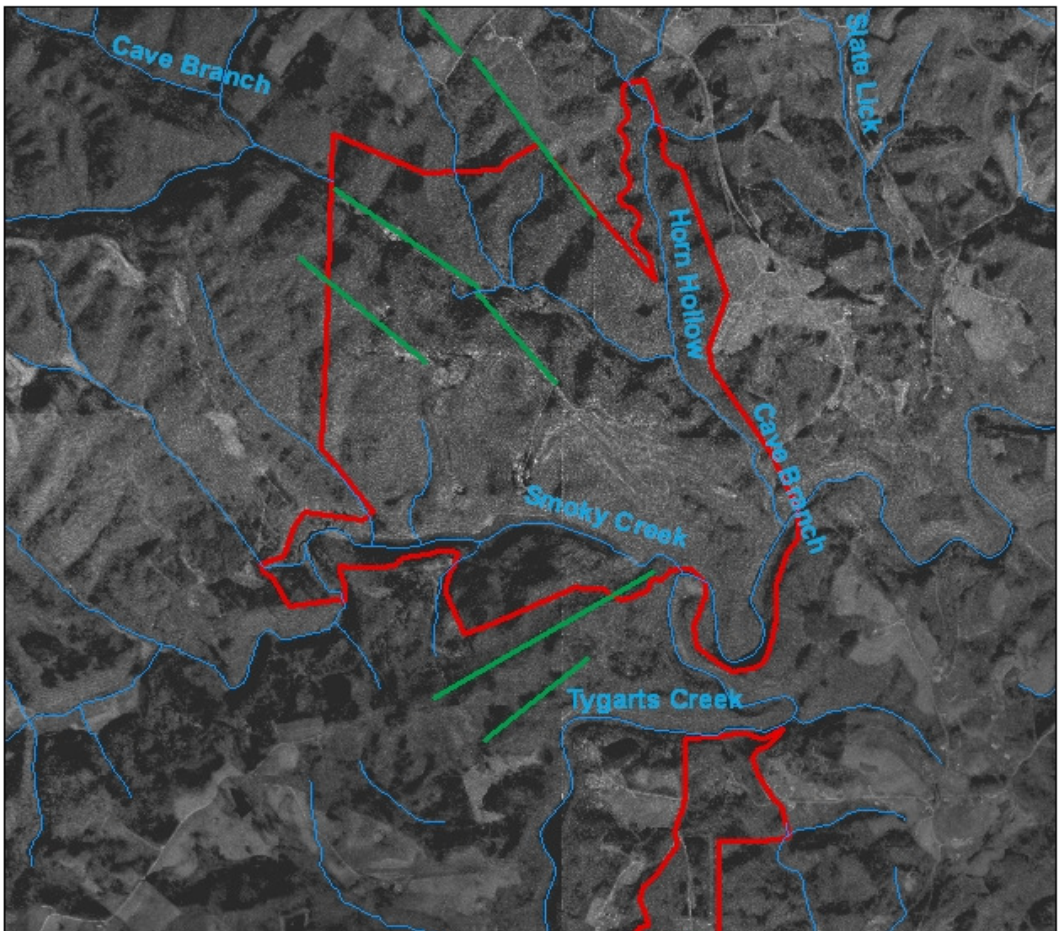

Figure 11. Lineaments detected. The lineaments are the green lines.

Sinkholes

In order to find sinkholes within the CCSRP, the same NIR filtered image was used. However, this time dark spots on the image were compared to topographic lows on a topographic map as well as where there are known pits or sinks. Several dark areas were identified in the image but many were discarded as a sinkhole because they were at a topographic high. The sinkholes found follow the same trend as the lineaments, rivers, and cave entrances (Figure 12).

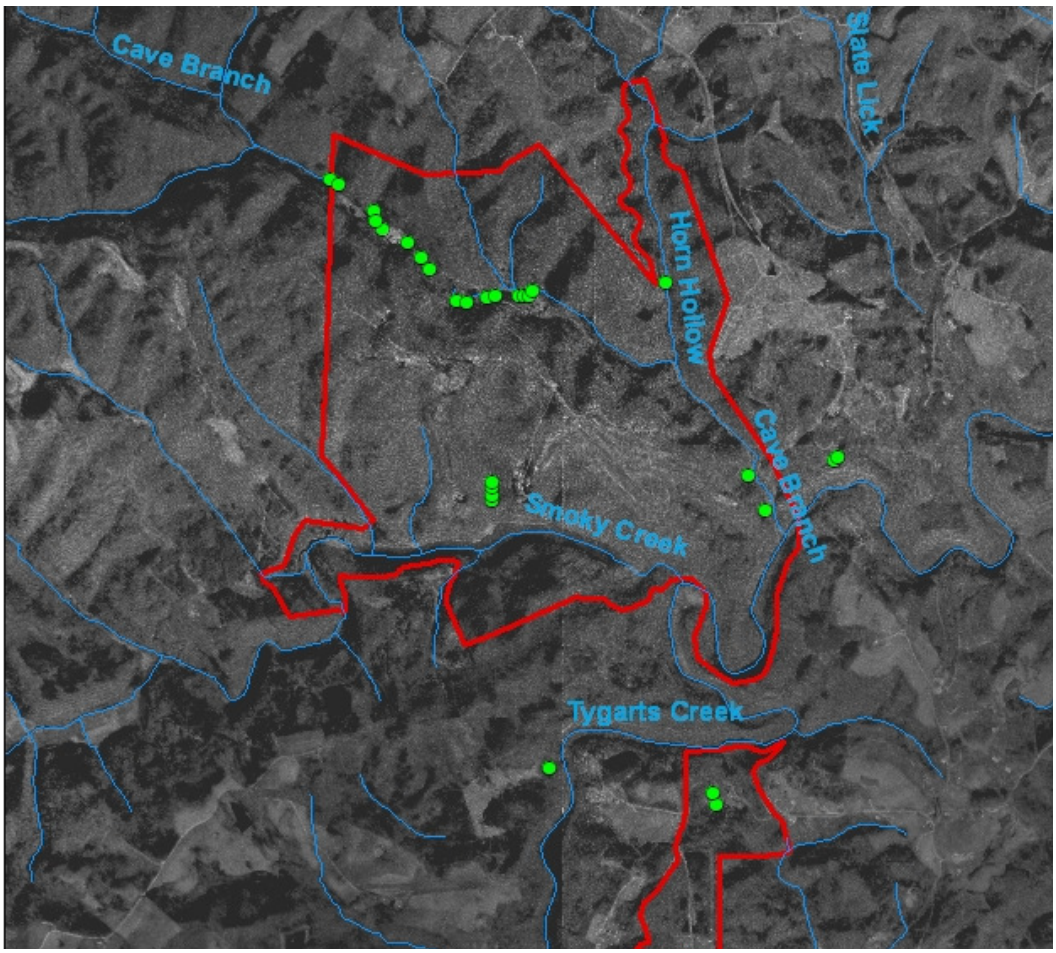

Figure 12. Sinkholes found in the CCSRP. The sinkholes are in green.

CHAPTER IV

THE CONCEPTUAL MODEL

Conceptual Model

The CCSRP contains over two hundred caves, pits, and sinkholes formed by the dissolution of limestone. The lineaments, cave entrances, and sinkholes have a northwest to southeast trend. The geologic bedding in the area also dips to the southeast due to the Waverly Arch with an axis that runs NNE to SSW. This uplift would cause the streams on the eastern side of the arch to have a general trend or flow to the southeast. Thus, it would make sense that the caves entrances and sinkholes to follow the same trend because these features form when the river waters erode the limestone and the direction of flow could be a preferential flow direction.

The lineaments detected trended on a northwest to southeast pattern in the northern part of the CCSRP and in the southern part of the CCSRP the lineaments trended on an almost southwest to northeast pattern. The lineaments in the northern portion are parallel to the rivers while the lineaments in the southern portion are perpendicular to the trend of the rivers but parallel to the Waverly Arch. Thus, the southern lineaments may be bedding plane fractures whereas the lineaments in the northern portion may be joints or fractures within the bedrock. It is also possible that the lineaments in the south are compliments to the northern lineaments and that there is just a lack of surface exposure to show the intersection of the two sets.

The stream network model showed that the streams in and around the CCSRP are continuous over the area even though they are not entirely

expressed at the surface and have a greater area of influence of erosion on the rocks below. The continuous nature can also be seen or checked in the field but is generally not seen on a map. The stream network model also helped to show the area of influence each stream has with CCSRP. In general, the closer a cave entrance was to the stream network, the lower in elevation it was and vice versa, the further away, the higher the elevation. So, as these streams erode their way down through the Mississippian limestone they widen out the valley walls and downcut from the cave entrances and caves that they have already been carved out. However, some of the higher elevation caves are in contact with the streams.

The cave entrances in the CCSRP have four defined levels at 231 to 232m (L1), 245m (L2), 258m to 260m (L3), and 270m (L4). L1 is contained within the St. Louis Limestone or the Borden Formation. L2 were formed in the Ste. Genevieve and St Louis Limestones. L3 cave entrances were formed out of eroded Ste Genevieve Limestone. L4 cave entrances were formed in the Ste. Genevieve and the Upper Member of the Newman Limestone. L5 are most likely contained within the Ste. Genevieve and the Upper Member Limestone of the Newman Formation. At Mammoth Caves, Palmer 1987, describe four main levels of caves at 152m, 168m, 180m, and 210m. The three lowest of the four levels were also in the Ste. Genevieve Limestone, which is laterally continuous to Mammoth. These formations dip to the northwest unlike in the CCSRP, which

the formations dip to the southeast because they are on the opposite side of an arch from Mammoth caves.

At Mammoth Caves the upper levels (210m-Level A and 180m-Level B) were determined to be formed in the Tertiary due to slow valley deepening and aggradation, while the lower levels (168m-Level C and 152m-Level D) were determined to be formed during the Quaternary due to sort intervals of base level stability (Palmer 1987). The age of Mammoth Cave was examined in 2001 by Granger et al using cosmogenic ^{26}Al and ^{10}Be which found that Level A (elevation from 190 to 210m with a mean elevation of 200m) and Level B (elevation from 175 to 190m with a mean elevation of 170-180m) were both formed prior to 3.25 Ma. Therefore Levels A and B were formed in the Pliocene. They also found that Level C (elevation from 165 to 175m with a mean elevation of 167m) was formed prior to 1.39 Ma. Level D (elevation from 150 to 158m with a mean elevation of 150m) was formed prior to 1.24 Ma. Therefore Levels C and D were formed in the Pleistocene. The Cumberland Plateau, which is east of Mammoth Cave and to the southwest of CCSRP also has a cave system that was age dated (Anthony and Granger 2004). The system also has four levels was dated using cosmogenic ^{26}Al and ^{10}Be. The anaylsis showed that the upper most level was formed prior to 5.7 and 3.5 Ma, the second level was formed between 3.5 and 2 Ma, the third level was formed between 2 and 1.5 Ma, and the fourth level was formed after 1.5 Ma. Thus, levels one and two formed in the Pliocene and levels three and four formed in the Pleistocene.

Mammoth Cave, Cumberland Plateau, and CCSRP are geographically close, contain many of the same Stratigraphic units, controlled ultimately by the base flow of the Ohio River. Thus, these cave systems should have a similar geologic history and experienced karstification at the same time. Each cave system has four cave levels. At Mammoth Cave and the Cumberland Plateau the highest caves levels formed first in the Pliocene and the bottom two or lowest cave levels formed last in the Pleistocene. Applying this to CCSRP, L1 (which is at the lowest elevations) could be said to be the youngest level and L4 (which is at the highest elevations) could be said to be the oldest level. Thus, the top levels could have been formed in the Pliocene while the lower levels would have formed in the Pleistocene.

Conclusion

The number of levels within the CCSRP shows that this area has experienced many changes in the stability of the water table. In addition, the rivers contained within the park have rapidly down cut through the Mississippian Limestones and have stalled out several times before reaching the elevations that they are seen at today. The Tygarts Creek has down cut to the Borden Formation and serves as the base level for the area. The tributaries of the Tygarts Creek are down cutting to the base level of the Tygarts Creek. In general, the upper reaches of the rivers (Box Canyon, Smoky Creek, Cave Branch, and Horn Hollow) are in the Upper Newman Limestone. The mid

reaches of these rivers are in the Ste. Genevieve Limestone and the lower reaches have down cut to the St. Louis Limestone. Therefore, these tributaries are still actively eroding and down cutting through the Mississippian Limestone in the area.

As for the future work needed for the area I would like to see the sinkholes or vertical features to be related to the streams because this research only looked at the horizontal features. I think it would be important to know whether the streams aided in the formation of sinkholes. In addition, I think that the age of the caves needs to be further researched to help decipher the absolute date the caves started forming.

References

Ali, S.A. and Pirasteh, S., 2004, Geological Applications of Landsat Enhanced Thematic Mapper (ETM) data and Geographic Information Systems (GIS): mapping and structural interpretation in south-west Iran, Zagros Structural Belt: International Journal of Remote Sensing, Vol. 25, No. 21, p 4715-4727.

Angel, J., Nelson, D., and Panno, S., 2004, Comparison of a New GIS-Based Technique and a Manual Method for Determining Sinkhole Density an Example from Illinois' Sinkhole Plain, Journal of Caves and Karst Studies, Vol, 66, No. 1, p. 9-17.

Annable, W.K. and Sudicky, E.A., 1999, On Predicting Contaminant Transport In Carbonate Terrains: Behavior and Prediction, Karst Modeling, ed. Palmer, A., Palmer, M., Sasowsky, I., Charlestown, West Virginia: Karst Waters Institute. Special Publication 5, p. 133-144

Anthony, D.M. and Granger, D.E., 2004, A Late Tertiary Origin for the Multileve Caves Along the Western Escarpment of the Cumberland Plateau, Tennessee and Kentucky, Established by Cosmogenic ^{26}Al and ^{10}Be: Journal of Cave and Karst Studies, Vol. 66, No. 2, p. 46-55.

Choi, J. and Engel, B., 2003, Real-Time Watershed Delineation System Using Web-GIS: Journal of Computing in Civil Engineering, Vol. 17, No. 3, p. 189-196.

Engel, A.S. and Engel, S.A., 2009, A Field Guide for the Karst of Carter Caves State Resort Park and the Surrounding Area, Northeastern Kentucky: Karst Waters Institute Special Publication 15, p. 154-171.

Erturk, A., Gurel, M., Baloch, M.A., Dikerier, T., Varol, E., Akbulut, N., and Tanik, A., 2006, Application of Watershed Modeling System (WMS) for Integrated Management of a Watershed In Turkey: Journal of Environmental Science and Health, Part A, Vol. 41, p. 2045-2056.

Florea, L. 2005, Using State-Wide GIS Data to Identify the Coincidence between Sinkholes and Geologic Structure: Journal of Caves and Karst Studies, Vol. 67, No. 2, p. 120-124.

Florea, L., Paylor, R., Simpson, L. and Gulley, J., 2002, Karst GIS Advances in Kentucky: Journal of Caves and Karst Studies, Vol. 64, No. 1, p. 58-62.

Gao, Y., Tipping, R.G., and Alexander, E.C., 2006, Applications of GIS and Database Technologies To Manage a Karst Feature Database: Journal of Cave and Karst Studies, Vol. 68, no. 3, p. 144-152.

Glennon, A., and Groves, C., 2002, An Examination of Perennial Stream Drainage Patterns within the Mammoth Cave Watershed, Kentucky: Journal of Cave and Karst Studies, Vol. 64, no. 1, p. 82-91.

Granger, D.E., Fabel, D., Palmer, A.N., 2001, Pliocene-Pleistocene Incision of the Green River, Kentucky, Determined from Radioactive Decay of Cosmogenic ^{26}Al and ^{10}Be In Mammoth Cave Sediments, GSA Bulletin, Vol. 113, No. 7, p. 825-836.

Hobbs, H. and Pender, M., 1985, The Horn Hollow Cave System, Carter County, Kentucky, Pholeos, Vol. 5, No. 2, p. 17-24.

Hung, L. and Dihn, N. 2002. Remote Sensing and GIS-Based Analysis of Cave Development in the Suoimuoi Catchment (Son La, NW Vietnam): Journal of Caves and Karst Studies. Vol. 64. No. 1. p. 23-33.

Janssen, R.E., 1953, The Teays River, Ancient Precursor of the East: The Scientific Monthly, Vol. 77, No. 6, p. 306-314.

Jenson, S.K. and Domingue, J.O., 1988, Extracting Topographic Structure from Digital Elevation Data for Geographic Information Systems Analysis: Photogrammetric Engineering and Remote Sensing, Vol. 54, No. 11, p. 1593- 1600.

Kentucky Geological Survey, 2008, Topographic maps: 24k, 7.5-minute quadrangles, State plane north and south, http://www.uky.edu/KGS/gis/mapimages.htm, Accessed October 12, 2008.

Litwin, L. and Andreychouk, V., 2008, Characteristics of high-mountain karst based on GIS and Remote Sensing: Environmental Geology, Vol. 54, p. 979-994.

Lo, C.P. and Yeung, A.K.W, 2006, *Concepts and Techniques of Geographic Information Systems.* 2nd edition. Upper Saddle River, NJ: Prentice Hall, p. 532.

McGrain, P., 1966, Geology of Carter and Cascade Caves Area, Kentucky Geological Survey, Special Publication 12, Series X, p. 1-32.

McNeil, B., Jasper, J., Luchsinger, D. and Rainsmier, M. 2002, Implementation and Application of GIS at Timpanogos Cave National Monument, Utah. Journal of Caves and Karst Studies. Vol. 64. No. 1. pp. 34- 37.

Mahler, B.J., Lynch, L., and Bennett, P.C., 1999, Mobile Sediment in Urbanizing Karst Aquifer: Implications for Contaminant Transport: Environmental Geology, Vol. 39, p. 25-38.

Martin, J.B. and Gordon, S.L., 2000, Groundwater Flow and Contaminant Transport in Carbonate Aquifers, A.A. Balkema, ed. Sasowsky, I.D. and Wicks, C.M., 64-93.

Ohms, R. and Reece, M., 2002, Using GIS to Manage Two Large Cave Systems, Wind and Jewel Caves, South Dakota: Journal of Caves and Karst Studies, Vol. 64, No. 1, p. 4-8.

Palmer, A., 1987, Cave Levels and Their Interpretations: NSS Bulletin, Vol. 49, p. 50-66.

Sahoo, P.K., Kumar, S., and Singh, R.P., 2000, Neotectonic study of Ganga and Yumuma tear faults, NW Himalaya, using remote sensing and GIS: International Journal of Remote Sensing, Vol. 25, No. 3, p499-518.

Saraf, A.K., Goyal, V.C., Negi, A.S., Roy, B. and Choudhary, P.R., 2000, Remote Sensing and GIS Techniques for the study of springs in a watershed in Garhwal in the Himalayas, India: International Journal of Remote Sensing, Vol. 21, No. 12, p2353-2361.

Seale, L.D., Florea, L.J., Vacher, H.L., and Brinkman R., 2008, Using ALSM to map sinkholes in the urbanized covered karst of Pinellas County, Florida-1, methodological considerations: Environmental Geology, Vol. 54, p. 995-1005.

Tierney, J., 1985, Caves of northeastern Kentucky (with special emphasis on Carter Caves State Park), *in* P. H. Dougherty, ed., Caves and Karst of Kentucky, v. Special Publication 12, Series XI: Lexington, KY, Kentucky Geological Survey, p. 78-85.

United States Geological Survey, 1999, National Elevation Dataset, seamless.usgs.gov, Accessed October12, 2008

Wang, L. and Liu, H., 2006, An Efficient Method for Identifying and Filling Surface Depressions in Digital Elevations Models for Hydrologic Analysis and Modeling: International Journal of Geographical Information Science, Vol. 20, No. 2, p. 193-213.

Woodside, J., 2008, Examination of the Relationship between Longitudinal Profile and Sediment Mobility within a Fluviokarst Stream System, Thesis: unpublished, 70p.

Yilmaz, I., 2006, GIS Based susceptibility mapping of Karst Depression in Gypsum: A Case Study from Sivas Basin (Turkey), Engineering Geology, Vol. 90, p. 89-103.

APPENDIX A

CARTER CAVES STATE RESORT AND PARK

ELEVATION DATA

Level 1

Cave Entrance	DEM elevation (m)
Hidden Cave	215
Natural Tunnel Annex Cave	215
Cliff Edge Cave	217
Counterloop Cave - East entrance	218
KBH Cave	219
Weeping Spring Cave	221
Cool James Cave - Lower entrance	221
Cave 1	221
Tygarts Saltpetre Cave - Main entrance	223
Jones Cave	226
Laurel Cave - Upper level entrance	226
Dam-In Cave	228
Lake Cave	228
Sinus Cave	228
Wet Crevice Cave - East entrance	228
Cascade Cave Karst window entrance	229
Natural Tunnel - West entrance	229
Cascade Cave Sport Portal	230
Laurel Cave - Upper entrance	230
H2O Cave - Lower entrance	230
Cave 2	230
Boat Dock Cave	231
Laurel Cave - Main entrance	231
Matt's Cave	231
Sandy Cave	231
Open Mouth Cave	231
Cascade Cave Backdoor	232
Cool James Cave - Middle entrance	232

Level 1 Continued

Cave Entrance	DEM elevation (m)
Cascade Cave Tourist entrance 2	232
Lower Old Homestead Cave	232
New Cave	232
AA Cave	233
H2O Cave - Upper entrance	233
Sandy (Cascade) Karst Window	233
Bodylength Cave	234
Uvula Cave	234

Mean	228
Median	230
Mode	231
Range	19
Minimum	215
Maximum	234
Count	36

Level 2

Cave Entrance	DEM elevation (m)
Cave 3	235
Green Trail Cave	235
Natural Tunnel - East entrance	235
Unnamed Cave East of Raven Bridge	236
Headwall Cave	236
Contact Cave	236
Watergate Cave	236
Cascade Cave Tourist exit	237
Salt Rock Cave	237
Cascade Cave North Cave	238
Hourglass Cave	238
Old Man's Cave	238
Lower Horn Hollow Cave	239
Cave Branch Cave - Lower entrance	239
Horn Hollow Window	239
Cliff Climb Cave	239
Cliff Crawl Spring Cave	240
Loop Cave	240
Tygarts Saltpetre Cave - West entrance	240
Little Arch Cave	241
Cliff Cave	241
Upper Horn Hollow Cave	242
Adams Creek Karst Window	242
Dome Cave	242
Katie's Cave	242
Cool James Cave - Upper entrance	242
Wet Crevice Cave - West entrance?	243
Shovel Cave	243
Bowel Cave	244
Cave 4	244
Walking Fern Cave	244
Cobble Crawl Cave - Lower entrance	245
Pinch-out Cave	245
Dead Air Cave	245

Level 2 continued

Cave Entrance	DEM elevation (m)
Upper Horn Hollow Cave II	245
Constipation Cave	245
Cascade Cave Tourist entrance 1	245
Hot Dog Cave	245
Old Homestead Karst Window	246
Root Cave	246
Adams Creek Cave	246
Burchett's Cave - Meander Crawl entrance?	246
Crawl-in-the-Wall Cave	246
Cobble Crawl Cave - Upper entrance	247
Burchett's Cave - Rat entrance	247
Mustard Cave	247
Copperhead Arch Cave - Breakdown entrance	247

Mean	246
Median	246
Mode	246
Range	12
Minimum	235
Maximum	247
Count	47

Level 3

Cave Entrance	DEM elevation (m)
Tire Creek Cave	249
River Bend II Cave - Front entrance	249
Boundary Cave - Streambed entrance	250
Triangle Cave	250
Tierney's Cave	251
Kiser Hollow Cave	252
Kiser Hollow Spring Cave	252
Rimstone Cave	253
Skylight Cave	254
Bio Cave	254
Blackbeard Cave	255
Liverwort Cave	255
Impossible Cave	256
Volcano Cave	256
Shagbark Cave	256
Possible Dig Cave	257
Smokey Bridge Cave	257
Bat Cave - Upper entrance	257
L Cave	257
Cave Branch Cave - Dry entrance	258
Cave Branch Cave - Upper entrance	258
X Cave - Cliff entrance	258
Bat Cave Annex	258
Moss Rock Cave	258
Icebox Cave	258
X Cave - Backdoor entrance south	259
Counterloop Cave - West entrance	259
Upper Old Homestead Cave	259
Winston's Crawl Cave	259
X Cave - Backdoor entrance north	259
Pick-up Sticks Cave	260
Copperhead Arch Cave - Main entrance	260
Saltpetre Cave - Cliff entrance	260
Cascade Cave Natural entrance	260
Unknown Cave Updrain from Dripping Moss Pit	260

Level 3 Continued

Cave Entrance	DEM elevation (m)
Rat Cave	260
Top of Cliff Cave	261
Welcome Center I Cave	261
Saltpetre Cave - Main entrance	261
Y Cave	262
River Bend I Cave	262
SR 182 Swallowhole Cave - Downstream	263
Pillar Cave	264
Lazy Fern Spring Cave	264
V Cave	265
Lost Cavern	265
Crack-by-the-Creek Cave	265
Boundary Cave - Upper end	266
Tight Crevice Cave	266

Mean	258
Median	258
Mode	258
Range	17
Minimum	249
Maximum	266
Count	49

Level 4

Cave Entrance	DEM elevation (m)
Coon-In-The-Crack Cave I	268
Bone Hole Cave - North entrance	268
SR 182 Swallowhole Cave - Upstream	269
Moon Cave - Main entrance	269
Turtle Cave	269
Bat Cave - Historic entrance	270
River Bend II Cave - Back entrance	270
Flood Cave	270
Bone Hole Cave - South entrance	270
X Cave - Tourist entrance	271
Teardrop Cave	271
Joan of Arch Cave	272
Earth Day Cave	274
Contact Rat Cave	274
Slope Cave	276
Jack-in-the-Pulpit Cave	276
Coon-In-The-Crack Cave II	278
Wilburn Cave	279
Stream Drain Cave	281
Canyon Cave	282
Burchett's Cave - Charlie Brown entrance	282
Coy's Cave	283
Suzanne No Show Cave	291
Burchett's Cave - Main entrance	298
Tygarts Creek Cave	298

Mean	276
Median	274
Mode	270
Range	30
Minimum	268
Maximum	298
Count	25

WSU ELEVATION DATA COMPARED TO DEM ELEVATION

LOCATION	WSU Field elevation (m)	DEM elevation (m)	Error (m)	Error Squared
847_BM_on_road_to_picnic_area	257.9	258.5	-0.6	0.36
bat_cave_entrance	240.2	252.1	-11.9	141.61
Bench_Mark_Gaurdrail_15	236.2	231.8	4.4	19.36
Bench_Mark_over_Natural_Birdge	260.6	258.5	2.1	4.41
boundary_cave_entrance	251.2	249.9	1.3	1.69
boundary_cave_entrance_sounding	245.1	249.9	-4.8	23.04
Bowl_Spring	239.6	243.5	-3.9	15.21
Cascade_Cave_entrance	238.4	232.6	5.8	33.64
Cascade_Cave_south_Entrance	246.3	245.1	1.2	1.44
cistern?_across_from_kiosk	249.3	250.2	-0.9	0.81
Cistern_at_Visitors_Center	249.6	250.2	-0.6	0.36
Cobble_Cave_DS_entrance	241.4	246.6	-5.2	27.04
Cobble_Cave_US_entrance	240.5	244.7	-4.2	17.64
entrance_upper_x	257.6	257.5	0.1	0.01
guardrail_15th_post_frm_dwnhill	225.2	231.8	-6.6	43.56
H2O_Cave_US_entrance	233.2	232.8	0.4	0.16
h2o_entrance	224.3	223.2	1.1	1.21
H2O_Outlet	224.3	223.2	1.1	1.21
H2O_Outlet_Conduit	229.5	230.2	-0.7	0.49
H2O_Outlet_Spring_flow	229.2	230.2	-1.0	1.00
Headwall_sink_between_ Fudge_Ripple_and_tic_tac_toe_caves	262.4	265.7	-3.3	10.89
HH_Cave_DS_entrance	239.9	238.8	1.1	1.21
HH_Inlet	242.9	239.2	3.7	13.69
Horn_Hollow_Cave_Ledge_Benchmak	242	238.8	3.2	10.24
Horn_Hollow_Dry_Creek_DWNS	236.8	239.1	-2.3	5.29
Horn_Hollow_Stream_Bedrock_ Before_Sink	237.4	239.1	-1.7	2.89
Jet_Pit_stadia_rod	259.1	255.6	3.5	12.25

LOCATION CONTINUED	WSU Field elevation (m)	DEM elevation (m)	Error (m)	Error Squared
Laurel_Cave	224.9	229.6	-4.7	22.09
Laurel_Cave_US_Entrance	235	232.4	2.6	6.76
Laurel_Entrance_DS	232.6	230.9	1.7	2.89
Lower_X_Cave	231	247.1	-16.1	259.21
middle_of_Laurel-H2O_sink	235	232.4	2.6	6.76
natural_bridge	245.1	250.5	-5.4	29.16
New_Cave	233.2	229.6	3.6	12.96
Rimstone_Entrance	249.3	246.3	3.0	9.00
saltpeter_cave_gate_entrance	258.2	260.9	-2.7	7.29
Sink_Hole_Betwean_rimstone_and_HH	250.5	248.4	2.1	4.41
Sink_Hole_on_Saddle	235.6	242.3	-6.7	44.89
Sinkhole_with_small_cave_ and_flowing_water	254.2	264.6	-10.4	108.16
Sm._cave_in_cliff_NW_of_HH_Str	249.9	239.5	10.4	108.16
small_entrance_near_pavilion	236.5	245.2	-8.7	75.69
Smokey_Bridge	248.9	255.5	-6.6	43.56
Surprise_Dome	246.6	235.2	11.4	129.96
swallet_on_east_valley_wall_ near_JET_pit_at_rock_outcrop	271	269.5	1.5	2.25
volcano_cave_entrance	254.8	256.9	-2.1	4.41

Root Mean Square Error	5.31

APPENDIX B

CARTER CAVES STATE RESORT AND PARK

DISTANCE TO STREAMS DATA

Level 1

Cave Entrance	Distance to Stream (m)
KBH Cave	0
Tygarts Saltpetre Cave - Main entrance	0
H2O Cave - Lower entrance	0
Laurel Cave - Main entrance	0
H2O Cave - Upper entrance	0
Sinus Cave	10
Cascade Cave Sport Portal	10
Open Mouth Cave	10
Cool James Cave - Middle entrance	10
Cliff Edge Cave	14
Jones Cave	14
Laurel Cave - Upper level entrance	14
Cascade Cave Karst window entrance	14
Cascade Cave Backdoor	14
Natural Tunnel Annex Cave	20
Laurel Cave - Upper entrance	20
Hidden Cave	22
Matt's Cave	22
Cascade Cave Tourist entrance 2	22
Natural Tunnel - West entrance	30
Cave 2	30
Bodylength Cave	30
Uvula Cave	30
Sandy Cave	32
New Cave	32
Sandy (Cascade) Karst Window	32
Weeping Spring Cave	36
Lake Cave	36

Level 1 Continued

Cave Entrance	Distance to Stream (m)
Boat Dock Cave	36
Lower Old Homestead Cave	36
AA Cave	41
Cave 1	42
Counterloop Cave - East entrance	45
Dam-In Cave	50
Wet Crevice Cave - East entrance	50
Cool James Cave - Lower entrance	54
Average Distance to stream for L1	24

Level 2

Cave Entrance	Distance to Stream (m)
Cave 3	0
Headwall Cave	0
Katie's Cave	0
Shovel Cave	0
Bowel Cave	0
Cave 4	0
Adams Creek Cave	0
Cascade Cave North Cave	10
Lower Horn Hollow Cave	10
Cliff Climb Cave	10
Adams Creek Karst Window	10
Wet Crevice Cave - West entrance?	10
Pinch-out Cave	10
Upper Horn Hollow Cave II	10
Constipation Cave	10
Old Homestead Karst Window	10
Mustard Cave	10
Copperhead Arch Cave - Breakdown entrance	10
Green Trail Cave	14
Tygarts Saltpetre Cave - West entrance	14
Cliff Cave	14
Horn Hollow Window	20
Hot Dog Cave	20
Burchett's Cave - Meander Crawl entrance?	20
Cascade Cave Tourist exit	22
Watergate Cave	28
Cool James Cave - Upper entrance	28
Cliff Crawl Spring Cave	30
Walking Fern Cave	30
Natural Tunnel - East entrance	36
Upper Horn Hollow Cave	36
Cobble Crawl Cave - Upper entrance	36
Burchett's Cave - Rat entrance	41
Little Arch Cave	42
Cave Branch Cave - Lower entrance	45

Level 2 continued

Cave Entrance	Distance to Stream (m)
Loop Cave	45
Crawl-in-the-Wall Cave	45
Unnamed Cave East of Raven Bridge	50
Hourglass Cave	50
Root Cave	50
Cobble Crawl Cave - Lower entrance	60
Contact Cave	64
Dead Air Cave	81
Dome Cave	82
Salt Rock Cave	94
Cascade Cave Tourist entrance 1	148
Old Man's Cave	184
Average Distance to stream for L2	33

Level 3

Cave Entrance	Distance to Stream (m)
Blackbeard Cave	0
Winston's Crawl Cave	0
Skylight Cave	10
Upper Old Homestead Cave	10
SR 182 Swallowhole Cave – Downstream	10
Lazy Fern Spring Cave	10
Boundary Cave - Upper end	10
Tight Crevice Cave	10
Bat Cave - Upper entrance	11
Impossible Cave	14
Smokey Bridge Cave	14
Icebox Cave	14
Rimstone Cave	20
Bio Cave	20
Shagbark Cave	20
Cave Branch Cave - Upper entrance	20
Y Cave	20
Boundary Cave - Streambed entrance	22
Triangle Cave	22
Volcano Cave	22
Pick-up Sticks Cave	28
Copperhead Arch Cave - Main entrance	28
Welcome Center I Cave	28
Moss Rock Cave	30
Saltpetre Cave - Cliff entrance	30
Cave Branch Cave - Dry entrance	32
X Cave - Cliff entrance	32
Top of Cliff Cave	32
Bat Cave Annex	36
Lost Cavern	36
Tire Creek Cave	40
Liverwort Cave	40
Unknown Cave Updrain from Dripping Moss Pit	41
Crack-by-the-Creek Cave	41
X Cave - Backdoor entrance south	50

Level 3 continued

Cave Entrance	Distance to Stream (m)
X Cave - Backdoor entrance north	50
Counterloop Cave - West entrance	57
Kiser Hollow Cave	58
Kiser Hollow Spring Cave	58
Saltpetre Cave - Main entrance	58
L Cave	63
River Bend I Cave	63
Rat Cave	80
Pillar Cave	80
V Cave	89
River Bend II Cave - Front entrance	110
Possible Dig Cave	149
Tierney's Cave	157
Cascade Cave Natural entrance	157
Average Distance to stream for L3	41

Level 4

Cave Entrance	Distance to Stream (m)
Teardrop Cave	0
Bone Hole Cave - North entrance	10
Bone Hole Cave - South entrance	10
Burchett's Cave - Charlie Brown entrance	10
SR 182 Swallowhole Cave – Upstream	20
Contact Rat Cave	20
Coy's Cave	28
Joan of Arch Cave	36
Slope Cave	40
Stream Drain Cave	40
Bat Cave - Historic entrance	41
Flood Cave	42
X Cave - Tourist entrance	51
Coon-In-The-Crack Cave I	67
Jack-in-the-Pulpit Cave	85
Coon-In-The-Crack Cave II	85
Burchett's Cave - Main entrance	89
Turtle Cave	99
Earth Day Cave	106
River Bend II Cave - Back entrance	122
Tygarts Creek Cave	130
Moon Cave - Main entrance	140
Suzanne No Show Cave	144
Canyon Cave	164
Wilburn Cave	210
Average Distance to stream for L4	72

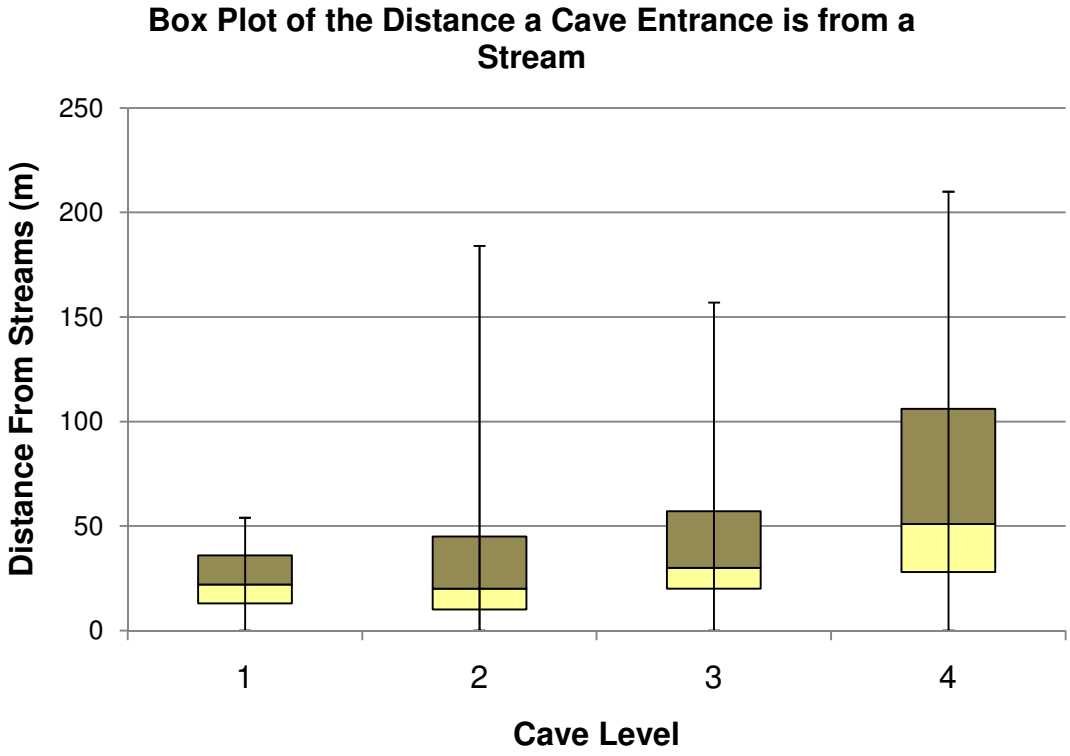
Box Plot of the Distance a Cave Entrance is from a Stream
Distance From Streams (m)
250
200
150
100
50
0
1
2
3
4
Cave Level